Sustained release of a p38 inhibitor from non-inflammatory microspheres inhibits cardiac dysfunction

JAY C. SY[1], GOKULAKRISHNAN SESHADRI[1], STEPHEN C. YANG[1], MILTON BROWN[1], TERESA OH[1], SERGEY DIKALOV[2], NIREN MURTHY[1] AND MICHAEL E. DAVIS[1,2]*

[1]Wallace H. Coulter Department of Biomedical Engineering, Emory University and Georgia Institute of Technology, Atlanta, Georgia 30322, USA
[2]Division of Cardiology, Emory University School of Medicine, Atlanta, Georgia 30322, USA
*e-mail: michael.davis@bme.emory.edu

Published online: 19 October 2008; doi:10.1038/nmat2299

Cardiac dysfunction following acute myocardial infarction is a major cause of death in the world and there is a compelling need for new therapeutic strategies. In this report we demonstrate that a direct cardiac injection of drug-loaded microparticles, formulated from the polymer poly(cyclohexane-1,4-diylacetone dimethylene ketal) (PCADK), improves cardiac function following myocardial infarction. Drug-delivery vehicles have great potential to improve the treatment of cardiac dysfunction by sustaining high concentrations of therapeutics within the damaged myocardium. PCADK is unique among currently used polymers in drug delivery in that its hydrolysis generates neutral degradation products. We show here that PCADK causes minimal tissue inflammatory response, thus enabling PCADK for the treatment of inflammatory diseases, such as cardiac dysfunction. PCADK holds great promise for treating myocardial infarction and other inflammatory diseases given its neutral, biocompatible degradation products and its ability to deliver a wide range of therapeutics.

The development of drug-delivery vehicles that can improve cardiac dysfunction following myocardial infarction (MI) remains a major challenge in the field of biomaterials. Following acute MI, an excessive inflammatory response is initiated in the myocardium, causing chronic elevation of inflammatory cytokines and reactive oxygen species, resulting in cardiac dysfunction[1–4]. A large number of clinically approved small molecule inhibitors have been identified that can suppress inflammation and have great potential for improving cardiac dysfunction. However, delivery remains a challenge, as many of these drugs require large doses and daily injections for efficacy and cause toxicity at these high doses[5–7]. Thus, drug-delivery vehicles that can sustain effective doses of therapeutics within the myocardium for weeks have the potential to slow or halt the progression of cardiac dysfunction[8]. Although biomaterials have been developed for treating cardiac dysfunction, these materials have been designed to deliver protein therapeutics and cells, and are not well suited for the controlled release of hydrophobic drugs, such as small molecule inhibitors, because of their large pore sizes[9]. Polyester-based microparticles do have the potential for delivering hydrophobic anti-inflammatory molecules; however, their use in cardiac drug delivery has not been fully investigated.

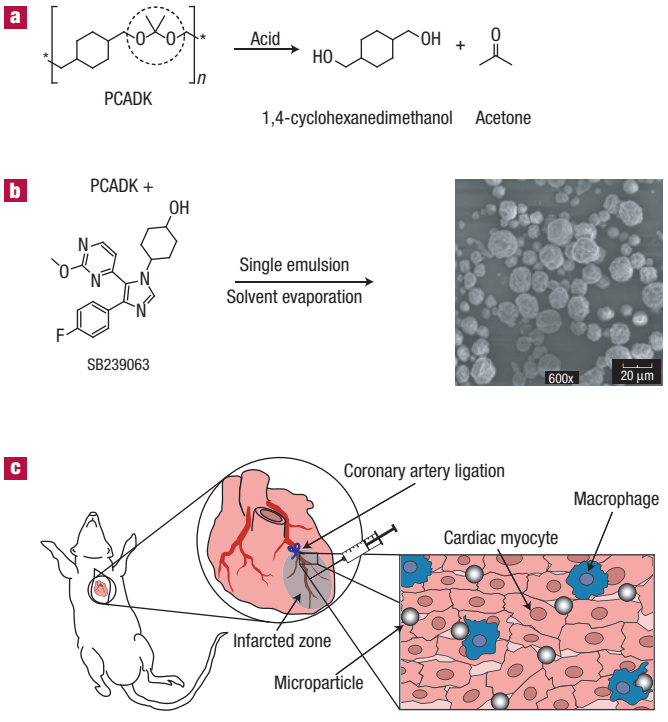

Figure 1 Polyketal microparticles—non-inflammatory polymer chemistry for drug delivery. a, Poly(cyclohexane-1,4-diylacetone dimethylene ketone) (PCADK) degrades to neutral, non-toxic products through the acid-catalysed hydrolysis of the ketal linkage (dotted circle). Acetone is an endogenous metabolite, and 1,4-cyclohexanedimethanol is Food and Drug Administration (FDA) approved as an indirect food additive. **b**, A single-emulsion/solvent-evaporation technique was used to produce large (~20 μm) microparticles loaded with SB239063. Particles were imaged using scanning electron microscopy. **c**, The left descending coronary artery was permanently ligated to create an infarcted zone. Microparticles were injected intramyocardially, where they released the encapsulated inhibitor within the infarct zone.

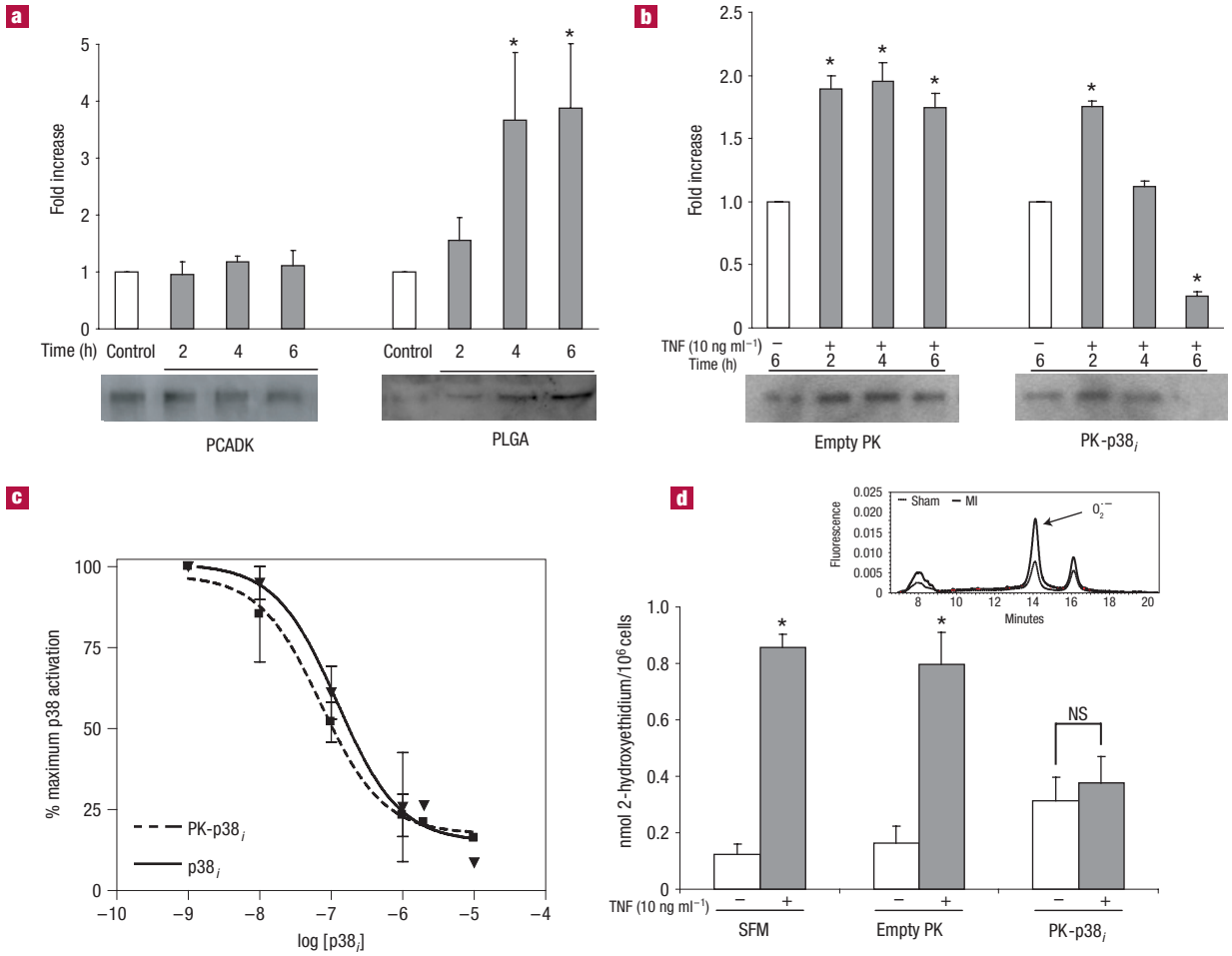

Figure 2 Macrophages are activated by PLGA microspheres *in vitro*, whereas PK-p38$_i$ treatment inhibits p38 activation. a, RAW 264.7 macrophages were treated with empty PCADK and PLGA particles for 2, 4 and 6 h. Densitometric evaluation (mean ± s.e.m.; $n = 3$) of Western blots (representative blot for phospho-p38 shown) demonstrate that PCADK did not elevate p38 phosphorylation at any time point. PLGA increased p38 phosphorylation in a time-dependent manner, resulting in a fourfold increase in activation at 4 and 6 h ($^*p < 0.05$ versus all groups; analysis of variance (ANOVA) followed by Tukey–Kramer post-test). **b**, Macrophages were treated with PK-p38$_i$ particles for the indicated time and stimulated with tumour necrosis factor-alpha (TNF-α). A time-dependent inhibition of phosphorylation was observed, with complete inhibition occurring at 4–6 h, and no effect seen with empty polyketal (PK) treatment (mean ± s.e.m., $n = 4$, $^*p < 0.05$ versus control, ANOVA followed by Tukey–Kramer post-test). **c**, Inhibition curves demonstrating similar dose–response profiles of the encapsulated and free inhibitor. Macrophages were stimulated with TNF-α following incubation with increasing doses of free or encapsulated inhibitor. There was no difference between treatments at any dose, and both showed similar IC_{50} (concentration at which half the response is inhibited) values. **d**, Superoxide production, a downstream effect of p38 activation, was measured using DHE-HPLC. HPLC traces were used to quantify the superoxide-specific oxidation product of dihydroethidium, 2-hydroxyethidium (sample traces from sham and infarcted animals shown, inset). No effect is seen with empty PK treatment, whereas PK-p38$_i$ reduced superoxide levels following TNF-α stimulation (mean ± s.e.m., $n = 4$, NS = not significant, $^*p < 0.05$ versus control; ANOVA followed by Tukey–Kramer post-test; SFM = serum-free medium).

In this work, we demonstrate that microspheres formulated from the polymer PCADK that encapsulate the p38 inhibitor SB239063 can improve the treatment of MI. PCADK is a recently developed, acid-sensitive (see Supplementary Information, Fig. S1a) polymer that has great potential for treating inflammatory diseases, such as MI, because it degrades into the neutral, excretable, FDA-approved compounds 1,4-cyclohexanedimethanol (approved by the FDA as an indirect food additive) and acetone (an endogenous compound with potential antioxidant properties) and thus should not exacerbate any existing inflammation[10,11] (Fig. 1a). Using an emulsion/solvent-evaporation procedure, we were able to encapsulate SB239063 using a single emulsion to produce microparticles of various sizes (Fig. 1b and Supplementary Information, Fig. S1b) owing to the compound's hydrophobicity (theoretical partition coefficient, $\log P = 3.28$, ACD/Labs Software, SciFinder Scholar). We focused on inhibiting the p38 mitogen-activated protein kinase pathway because of its central importance in activating macrophages and its role in inducing apoptosis in cardiomyocytes[12–17]. We therefore hypothesized that a direct injection of large PCADK–SB239063 microparticles, 10–20 μm in diameter, would be retained in the myocardium and slowly release the drug over the course of weeks, inhibiting p38 activation in many cell types. Additionally, this strategy would also be effective in inhibiting p38 activation in macrophages, as macrophages can phagocytose small particles and fragments of larger particles, thus releasing the inhibitor intracellularly (Fig. 1c).

Delivery vehicles, and their degradation by-products, can potentially cause the activation of inflammatory pathways

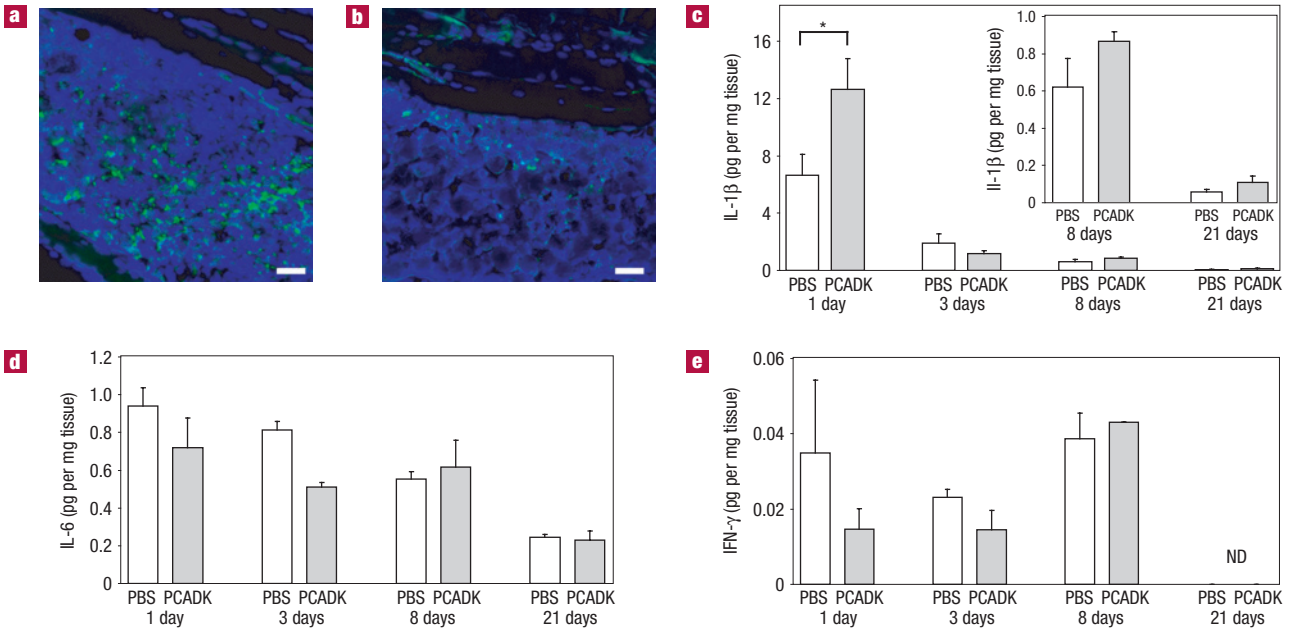

Figure 3 PCADK microparticles demonstrate little inflammatory response following intramuscular injections. Rats were injected with a high dose (50 mg ml^{-1}) of empty polymer microparticles. **a**,**b**, Histological sections were made and stained with 4′,6-diamidino-2-phenylindole for nuclei (blue) and CD-45, an inflammatory-cell-specific marker (green). Tissue injected with PLGA microspheres (**a**) shows a large influx of inflammatory cells, whereas tissue injected with PCADK microspheres (**b**) has little CD-45-positive staining. Scale bars = 100 μm. **c**–**e**, In a separate study, cytokine levels were measured in muscle tissue following an injection of 1 mg of PCADK particles or phosphate-buffered saline (PBS) using a multiplex assay. **c**, Injection of 1 mg of PCADK particles into the legs of rats leads to a slight elevation of interleukin-1β (IL-1β) at day 1. At days 8, 14 and 21 following surgery, PCADK particles do not elevate IL-1β above basal levels. **(d)** PCADK particles do not elevate IL-6 levels at any time point following injection of 1 mg of PCADK particles. **e**, Interferon-gamma (IFN-γ) levels are not affected by PCADK particles. IFN-γ was not detected by the Bioplex assay at 21 days (ND). (mean ± s.e.m., $^*p < 0.05$ versus PBS, Student's *t*-test).

in macrophages, and this is a critical issue limiting the use of microparticles for the treatment of inflammatory diseases. We therefore investigated whether degradation of PCADK microparticles by macrophages caused the activation of p38 itself and compared this with the response to poly(lactic-co-glycolic acid) (PLGA) microparticles as a control. Macrophages were incubated with PCADK or PLGA microparticles (PCADK, 19.2 ± 7.3 μm; PLGA, 17.9 ± 6.7 μm) for 2, 4 or 6 h, and examined for p38 phosphorylation by Western blotting. Figure 2a demonstrates that PLGA caused a time-dependent increase in p38 phosphorylation, suggesting elicitation of inflammatory pathways, whereas PCADK did not. These data agree with published reports showing that PLGA treatment increases inflammatory cytokine production in cultured cells[18,19], and also demonstrates that PCADK has potential as a drug-delivery vehicle designed to deliver anti-inflammatory drugs.

We therefore investigated the ability of PCADK microparticles to encapsulate the p38 inhibitor SB239063, and the bioactivity of these microparticles (PK-p38$_i$). The encapsulation efficiency of SB239063 was 44.4 ± 6.0%, and PK-p38$_i$ microparticles had 3–5 μg of inhibitor per mg of PCADK. To test bioactivity, macrophages were treated with either PK-p38$_i$ or empty PCADK particles (PK) for 2, 4 or 6 h, washed and stimulated for 20 min with TNF-α. As the representative blot and grouped data demonstrate, PK-p38$_i$, but not PK, prevented p38 phosphorylation by TNF-α stimulation in a time-dependent manner (Fig. 2b). Additionally, both the free inhibitor and PK-p38$_i$ demonstrated similar dose–response profiles, suggesting little loss of SB239063 activity in PK-p38$_i$ microparticles (Fig. 2c). The release half-life of SB239063 from PCADK microparticles is 7 days at pH 7.4, and thus on the basis of these release kinetics only 1.9% of encapsulated SB239063 (120 pmol) would be released into the extracellular media in our experiment on the 6 h cell culture. These results suggest that macrophages play an active role in accelerating the release of SB239063 from PK-p38$_i$ microparticles, either through phagocytosis of the microparticles, leading to intracellular release of the inhibitor, or through fusion of their phagosomes with the microparticles, leading to extracellular release of the inhibitor. Similar experiments with cultured neonatal cardiac myocytes, non-phagocytic cells, showed no inhibition of TNF-α-stimulated p38 phosphorylation, suggesting that passive hydrolysis alone cannot account for this inhibitory effect (see Supplementary Information, Fig. S2).

We also investigated whether PK-p38$_i$ microparticles could reduce downstream inflammatory effectors, in particular superoxide. Cultured macrophages were incubated with PK-p38$_i$ microparticles or empty PK microparticles, stimulated with TNF-α and then assayed for extracellular superoxide production. Superoxide production was quantified by measuring accumulation of a superoxide-specific oxidation product of dihydroethidium, 2-hydroxyethidium, by high-performance liquid chromatography (DHE-HPLC)[20,21]. As the data in Fig. 2d demonstrate, PK-p38$_i$ pretreatment reduced TNF-α-induced superoxide production, whereas PK had no effect. These data demonstrate that PK-p38$_i$ is active in reducing p38 phosphorylation, as well as clinically relevant p38-dependent second-messenger generation.

A key issue involving microparticle drug-delivery systems is the foreign-body response by the host immune system; in general, immune cells are recruited to the area of the microparticles and remain there until the microparticles are metabolized and

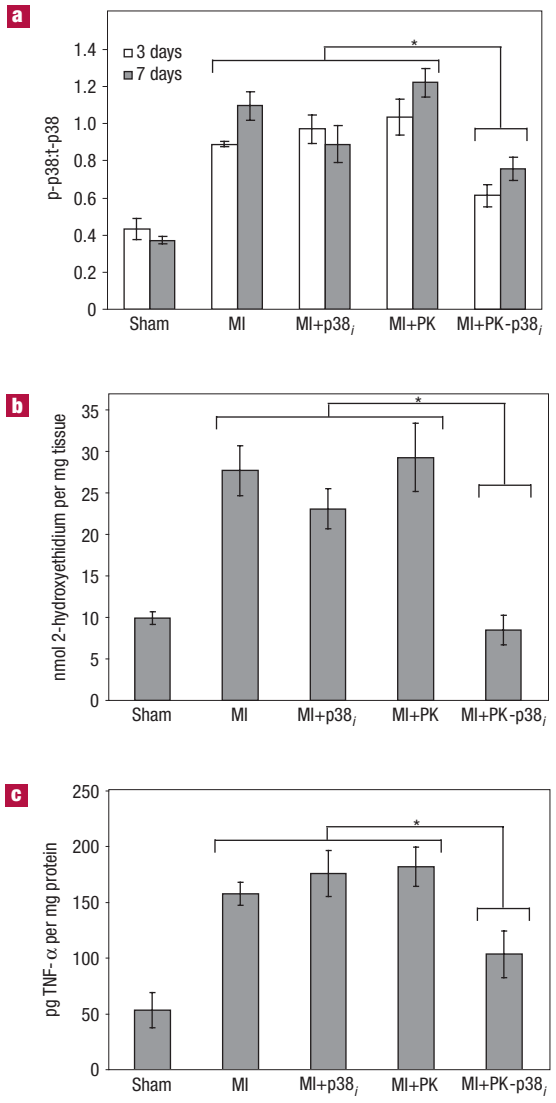

Figure 4 PK-p38$_i$ particles inhibit p38 phosphorylation, superoxide production and TNF-α production *in vivo* following infarction. a, PK-p38$_i$ treatment inhibited phosphorylation of p38 at three and seven days in the infarct zone, whereas free inhibitor (p38$_i$) or empty particles had no effect on phosphorylation at either time point (mean $\pm$ s.e.m., $n \geq 4$, $^*p < 0.05$ versus other treatment groups, ANOVA followed by Tukey–Kramer post-test; MI = myocardial infarction). **b**, Infarct zone tissue at three days was analysed for superoxide using DHE-HPLC. MI alone, free inhibitor and empty particles had significantly greater superoxide levels compared with sham, whereas PK-p38$_i$ decreased the amount of superoxide produced (mean $\pm$ s.e.m., $n \geq 4$, $^*p < 0.05$ versus other treatment groups, ANOVA followed by Tukey–Kramer post-test). **c**, The inflammatory cytokine TNF-α was measured in the infarcted zone by enzyme-linked immunosorbent assay three days postsurgery. MI alone, free inhibitor and empty particles had significantly greater amounts of TNF-α, whereas PK-p38$_i$ treatment reduced TNF-α levels nearly twofold (mean $\pm$ s.e.m., $n \geq 4$; $^*p < 0.05$ versus other treatment groups, ANOVA followed by Tukey–Kramer post-test).

phagocytosed, thus compromising the microparticle's function. The foreign-body response is particularly severe with particles that have acidic degradation products. In contrast, PCADK may minimize the foreign-body response because it generates neutral degradation products. We therefore compared the tissue biocompatibility of PCADK and PLGA microparticles. Mice were subjected to an intramuscular injection of size-matched PLGA or PCADK microparticles (50 mg ml^{-1}) and killed at 3 days, and histological sections of the injection site were made and stained for CD45, an inflammatory-cell marker. Figure 3a demonstrates that PLGA microspheres generated a large influx of CD45-positive cells (Fig. 3a), in agreement with previous studies demonstrating *in vivo* inflammation associated with PLGA delivery[22]. In contrast, PCADK microparticles caused very little recruitment of CD45-positive cells (Fig. 3b). We further investigated the inflammatory response to PCADK microparticles with quantitative cytokine analysis. Mice were subjected to an intramuscular injection of either saline (vehicle) or PCADK microparticles (10 mg ml^{-1}), and leg muscles were harvested at acute and chronic time points (1, 3, 8 and 21 days). We found that, although PCADK briefly increased levels of interleukin-1β (IL-1β) levels at day 1, there was no significant increase subsequently (Fig. 3c). Additionally, there was no significant increase in IL-6 (Fig. 3d) or interferon-gamma (Fig. 3e) at any time point, and levels of TNF-α and IL-12 were below detection limits (data not shown). These data suggest that PCADK microparticles do not induce an inflammatory response at concentrations far exceeding those needed for drug-delivery applications, and can therefore be used as a delivery vehicle for the treatment of inflammatory diseases.

PK-p38$_i$ microparticles were tested in a rat model of MI, as described in the methods section[23]. In preliminary experiments, we determined that PCADK microparticles with diameters of 15–20 μm remained in the myocardium for several days, most likely because their size precluded them from being carried away in the microcirculation (see Supplementary Information, Fig. S3). Following coronary-artery ligation, treatments were injected intramyocardially in a randomized and double-blind fashion (100 μl). Treatment conditions were vehicle, free inhibitor (2 μM), PK (0.5 mg particle ml^{-1}) or PK-p38$_i$ (0.5 mg ml^{-1} corresponding to 2 μM SB239063) injected directly into the left-ventricular free wall. At three and seven days following ligation, treatment with PK-p38$_i$ significantly inhibited p38 phosphorylation within the infarct zone, whereas free inhibitor and PK had no effect (Fig. 4a). These data suggest that PK-p38$_i$ is able to provide sustained p38 inhibition in the myocardium for at least seven days. Free SB239063 injections were not effective in inhibiting p38 phosphorylation, probably because the free inhibitor diffused away rapidly. Because chronic p38 inhibition has been shown to reduce levels of superoxide during heart failure[24], infarct zone tissue from three day samples was also analysed for the production of superoxide using DHE-HPLC. As the grouped data in Fig. 4b demonstrate, PK-p38$_i$ treatment significantly reduced superoxide levels, whereas free inhibitor and PK had no effect. Another downstream product of p38 activation, TNF-α production, was measured, and similarly only PK-p38$_i$ treatment was able to significantly reduce levels of this inflammatory cytokine (Fig. 4c).

In addition to *in vivo* findings supporting our *in vitro* biochemical data, we also measured the functional outcome of microparticle treatments in separate randomized and double-blind studies. We compared several treatment groups in these functional experiments: sham, MI, PK and PK-p38$_i$, as well as a separate randomized and blind study with PLGA and PLGA microparticles loaded with SB239063 (PLGA-p38$_i$). PLGA and PCADK delivery vehicles were compared in order to determine whether microparticle chemistry had an influence on therapeutic efficacy *in vivo*. PLGA-p38$_i$ and PK-p38$_i$ microparticles were similar in size (mean and distribution), loading efficiency and release kinetics (see Supplementary Information, Fig. S4). Cardiac function was assessed using magnetic resonance imaging and echocardiography 7 and 21 days postinfarction and dimensions of

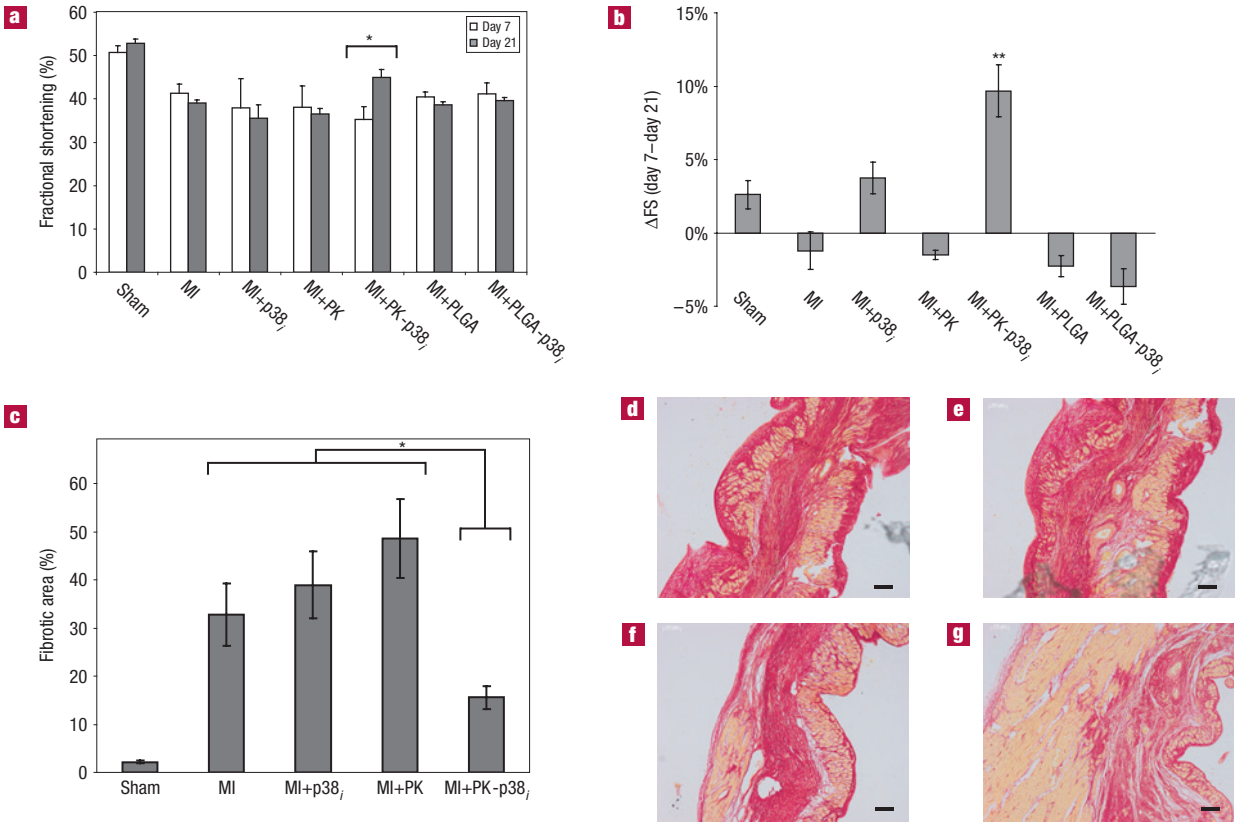

Figure 5 PK-p38$_i$ therapy results in improved cardiac function and reduced fibrosis. a, Dimensions of the left ventricle were measured at systole and diastole using magnetic resonance imaging at day 7 and day 21 post occlusion. PK-p38$_i$ showed a statistically significant difference between days 7 and 21, whereas all other treatments did not reach significance (mean $\pm$ s.e.m., $n \geq 4$, $^{*}p < 0.05$, repeated-measures ANOVA). In addition, PK-p38$_i$ fractional shortening was significantly higher on day 21 compared with MI alone and all other treatment groups (ANOVA followed by Tukey–Kramer post-test). **b**, Fractional shortening was measured and expressed as an absolute percentage difference between days 7 and 21. A positive value represents an improvement in cardiac function between days 7 and 21, whereas negative values represent progression of cardiac dysfunction. PK-p38$_i$ treatment showed a significant 10% improvement (absolute value) in cardiac function, whereas PLGA-p38$_i$ treatment did not inhibit cardiac dysfunction (mean $\pm$ s.e.m., $n \geq 4$, $^{**}p < 0.001$ versus all groups). **c**, The left-ventricular free wall was analysed histologically in at least three serial sections for fibrosis using a collagen-specific Picrosirius Red stain. MI-alone, free-inhibitor and empty-particle treatments had significant increases in fibrosis compared with sham operation. PK-p38$_i$ treatment reduced fibrotic area by more than half, though not completely to sham levels (mean $\pm$ s.e.m., $n \geq 4$, $^{*}p < 0.05$ versus other treatment groups, ANOVA followed by Tukey–Kramer post-test). **d–g**, Representative Picrosirius Red images of MI (**d**), MI + free inhibitor (**e**), MI + PK (**f**) and MI + PK-p38$_i$ (**g**) treatment are shown (scale bar: 200 μm).

the heart were measured in a double-blind manner. Although our biochemical data would suggest an immediate effect on function, we found no significant improvement with any treatment at seven days postinfarction (Fig. 5a; white bars). At 21 days, however, there was a significant improvement in fractional shortening in PK-p38$_i$-treated rats, whereas no effect was seen with free inhibitor, PK, PLGA or PLGA-p38$_i$ particles when compared with seven-day data (Fig. 5a; grey bars). Additionally, raw fractional shortening data on day 21 were significantly higher with PK-p38$_i$ treatment compared with MI alone and all other treatment groups (PK, p38$_i$, PLGA, PLGA-p38$_i$). To highlight this improvement over time, we expressed this as a difference in fractional shortening from 7 to 21 days, demonstrating that, although there was no initial improvement, sustained p38 inhibition slowed the progression of the dysfunction, even demonstrating improvement over time (Fig. 5b). We believe this can be explained by the fact that significant damage from MI by apoptosis and necrosis is done within the first 24–48 h (ref. 25). As the half-life of our particles is approximately 7 days, it is likely that the inhibitor was not released fast enough to affect this early time point.

Given that the effect on function was not seen early, we hypothesized that prolonged p38 inhibition was having an effect on the development of fibrosis[26,27]. Histological sections were made from the rats at 21 days postinfarction and stained for collagen using Picrosirius Red. Digital images of the sections were captured and quantified manually in a blind manner (Fig. 5c). Untreated MI and free-inhibitor and PK-particle treatments had significantly more fibrosis than sham-operated animals (Fig. 5d–f). Treatment with PK-p38$_i$, however, resulted in significantly less fibrosis in comparison with other treatment conditions (Fig. 5g). These data, taken together with the functional data, suggest that a single injection of PK-p38$_i$ microparticles reduced fibrosis and reversed progression of cardiac dysfunction following MI.

There is a compelling need for development of new biomaterials that can improve the treatment of cardiac dysfunction. In this letter, we demonstrate that the polyketal PCADK has the biocompatibility and controlled-release properties needed for treating inflammatory diseases. PCADK microparticles do not induce an inflammatory response *in vitro* or *in vivo*, and can therefore reside in inflamed tissue and act as a controlled-release reservoir for SB239063, with

a release half-life of 7 days for SB239063 at neutral pH values. We also demonstrate that delivery of PCADK microparticles loaded with SB239063 results in prolonged reduction of inflammatory signalling and eventual increased functional outcome from a single injection. In a direct comparison with PLGA, only loaded PCADK microparticles significantly improved function over time. On the basis of these results, we anticipate numerous applications of PCADK for treatment of myocardial infarction and other inflammatory diseases.

MATERIALS AND METHODS

POLYKETAL SYNTHESIS AND PARTICLE PREPARATION

PCADK was synthesized as described in ref. 11. Briefly, 1,4-cyclohexanedimethanol was reacted with 2,2-dimethoxypropane in an acetal exchange reaction. First, 1,4-cyclohexanedimenthanol was dissolved in benzene and brought to 100 °C with constant stirring. A solution of *p*-toluenesulphonic acid in ethyl acetate was added to the reaction flask in order to catalyse the reaction. The ethyl acetate was allowed to boil off, and distilled 2,2-dimethoxypropane was added to the benzene solution in an equimolar ratio to 1,4-cyclohexanedimethanol, initiating the polymerization reaction. Additional doses of 2,2-dimethoxypropane and benzene were subsequently added to the reaction dropwise to the reaction flask via a metering funnel to compensate for the 2,2-dimethoxypropane and benzene that had been distilled off. After 8 h, the reaction was stopped by addition of 500 µl of triethylamine. The polymer was isolated by precipitation in cold hexane (stored at −20 °C) followed by vacuum filtration. The molecular weight of the resulting polymer was approximately 6 kDa with a mean polydispersity of 1.923. All reagents were purchased from Sigma-Aldrich. 2,2-dimethoxypropane and benzene were distilled before use. *p*-toluenesulphonic acid was recrystallized before use. All other reagents were used as received.

Polyketal particles loaded with SB239063 (Axxora) (PK-p38$_i$) were generated using an emulsion/solvent-evaporation technique. 500 µg of inhibitor and 50 mg of PCADK were dissolved in 500 µl of dichloromethane. The polymer solution was then added to 5 ml of 4% PVA and homogenized at a low speed for 60 s. The resulting emulsion was transferred to 30 ml of 1% PVA and stirred at approximately 100 r.p.m. for 4 h to allow for evaporation of dichloromethane and solidification of microparticles. The particles were then centrifuged and washed with deionized water three times to remove residual PVA. The suspension was then frozen in liquid nitrogen and lyophilized to produce a free-flowing powder.

POLY(LACTIC-CO-GLYCOLIC ACID) PROPERTIES

PLGA (Resomer RG 503 H, 48:52 lactide:glycolide, 35.4 kDa, polydispersity 2.5, Boehringer Ingelheim) was used as received. Microparticles containing SB239063 were made with the same protocol as for PCADK particles and generated particles with similar inhibitor contents, sizes and release kinetics.

SB239063 LOADING AND RELEASE CHARACTERIZATION

PCADK particles containing SB239063 and corresponding empty particles were hydrolysed overnight in 1 N HCl at 65 °C. The resulting solution was measured at 320 nm and loading efficiencies calculated from a previously determined standard curve (correlation coefficient, $r^2 = 0.99$).

Release studies were conducted *in vitro* by suspending particles at a concentration of 1 mg ml^{-1} in PBS (pH 7.4) or 100 mM acetic acid (pH 4.5). One millilitre aliquots were made in microcentrifuge tubes and kept at 37 °C under constant agitation. At the designated time points, tubes were centrifuged and 200 µl of the supernatant withdrawn for analysis. Fresh buffer was replaced before vortexing to resuspend the particles. At the end of the release studies, the remaining polymers were centrifuged, supernatant removed and 1 N HCl added to hydrolyse the microparticles. Unreleased SB239063 was quantified spectrophotometrically and used to calculate the percentage of inhibitor released at each time point.

MACROPHAGE CULTURE

RAW264.7 macrophages were maintained in DMEM (Fisher) supplemented with 10% fetal bovine serum (Hyclone), L-glutamine and penicillin–streptomycin (Invitrogen). For experiments involving TNF-α stimulation, cells were plated at confluence 18 h before experiments in SFM (DMEM supplemented with L-glutamine and penicillin–streptomycin). Media were then aspirated and replaced with treatment media containing either SB239063 dissolved in DMSO, neat DMSO as a control or polyketal microparticles. Cells were preincubated with the treatment for the indicated time and washed with fresh SFM before being exposed to 10 ng ml^{-1} TNF-α (Sigma).

BIOPLEX CYTOKINE ANALYSIS AND INFLAMMATION STUDIES

C57BL6 adult mice (Charles River) were anaesthetized under isoflurane (1–3%, Charles River). Thighs were shaved and skin was incised to expose the muscle. For cytokine measurements, muscle was injected with 1 mg of polymer (100 µl of 10 mg ml^{-1} solution in sterile saline). The contralateral leg was injected with saline as a control. For immunohistochemical analysis 5 mg (100 µl of 50 mg ml^{-1} solution in sterile saline) was injected into the muscle. At the designated intervals, mice were killed with CO_2 and the leg muscles exposed. Approximately 50 mg of muscle was removed at the injection site and processed.

For cytokine analysis, tissue was frozen in liquid nitrogen and homogenized in cell-lysis buffer (Bio-Rad) according to the manufacturer's instructions. Briefly, tissue was homogenized in 0.5 ml of lysis buffer and sonicated to ensure full disruption of tissue. The homogenate was centrifuged and supernatant incubated with X-Plex multiplex beads (Bio-Rad) according to the manufacturer's instructions and analysed on a Bio-Rad Bioplex system.

For immunohistochemical analysis, tissue was fixed in 4% paraformaldehyde (Sigma) and embedded in paraffin. Histological sections were made and stained with FITC-conjugated anti-CD-45 antibody (eBiosciences) using standard immunohistochemical techniques. 4′,6-diamidino-2-phenylindole was used to visualize nuclei in the sections. Slides were imaged under fluorescence microscopy and digital images of the sections saved.

All animal experiments were approved by the Emory University Institutional Animal Care and Use Committee (protocol 188-2006).

RAT MYOCARDIAL INFARCTION MODEL

Adult male Sprague-Dawley rats (obtained from Charles River) weighing 250 g were subjected to MI/injection surgeries in a randomized and double-blind manner. Briefly, the animals were anaesthetized (1–3% isoflurane, Webster Veterinary) and, following tracheal intubation, hearts were exposed by separation of the ribs. Myocardial infarction was carried out by ligation of the left anterior descending coronary artery. Immediately after coronary artery ligation, polyketals (100 µl) were injected into the infarct zone through a 30-gauge needle while the heart was beating. Following injection, the chests were closed and animals allowed to recover on a heating pad. At the indicated time points, magnetic resonance imaging was carried out and data analysed in a blind manner. For immunohistological evaluation, hearts were harvested and fixed in 4% paraformaldehyde. Following dehydration, hearts were embedded in paraffin and 5 µm sections were made.

WESTERN ANALYSIS

Cell (250 µg) or tissue (500 µg) protein homogenates were incubated with an antibody against total p38 (Cell Signaling) overnight at 4 °C, before 2 h incubation with Protein-A agarose beads (Sigma). Beads were washed and boiled in sample buffer before loading on a 12% polyacrylamide–SDS gel. Proteins were transferred to a polyvinylidene fluoride membrane (Bio-Rad) and blots probed with an antibody for phospho-specific p38 (Cell Signaling). Films were scanned and quantified using Image J software.

QUANTIFICATION OF SUPEROXIDE VIA DHE-HPLC

To determine levels of superoxide in cells and tissues, a novel method described recently was used. DHE is a commonly used immunohistochemical marker to measure superoxide in tissues. However, when DHE is oxidized by superoxide, it becomes impermeable to cells. Therefore, any DHE oxidized in the extracellular space will remain in the incubation medium. This oxidation product, 2-hydroxyethidium, has a different retention from ethidium and can be quantified by HPLC with fluorescence detection[28].

To detect tissue superoxide following MI in rats, the left ventricular free wall was harvested at the indicated time point and equal-sized pieces were incubated at 37 °C in 1 ml of Krebs–HEPES buffer (pH = 7.35) containing 50 µM dihydroethidium (Invitrogen) for 30 min. Following incubation, buffer was syringe filtered and 100 µl placed in a tube containing 300 µl methanol. The sample was loaded on a C18 column for reverse-phase HPLC analysis using an acetonitrile gradient and data were normalized to wet tissue weight.

For cell-culture experiments, macrophages were incubated with polyketals for the indicated time period. Following polyketal pretreatment, cells were incubated with 10 ng ml^{-1} TNF-α for 5 min in Krebs–HEPES buffer at 37 °C, before addition of 25 µM dihydroethidium for 20 min. Buffer was collected and analysed in a manner similar to tissue studies.

TUMOUR NECROSIS FACTOR-ALPHA MEASUREMENT

Protein homogenates were evaluated for TNF-α levels by enzyme-linked immunosorbent assay (eBiosciences) according to the manufacturer's protocol and normalized to protein levels determined by Bradford assay.

COLLAGEN EVALUATION

Collagen deposition was determined by Picrosirius Red (Sigma) staining as previously described[29].

STATISTICAL EVALUATION

Treatment groups were analysed for statistical significance with GraphPad Prism software using post-test analysis where necessary.

Received 31 January 2008; accepted 22 September 2008; published 19 October 2008.

References

1. Anversa, P. Myocyte death in the pathological heart. *Circ. Res.* **86**, 121–124 (2000).
2. Anversa, P., Leri, A. & Kajstura, J. Cardiac regeneration. *J. Am. Coll. Cardiol.* **47**, 1769–1776 (2006).
3. Bolli, R. Oxygen-derived free radicals and myocardial reperfusion injury: An overview. *Cardiovasc. Drugs ther.* **5**, 249–268 (1991).
4. Bolli, R. *et al.* Direct evidence that oxygen-derived free radicals contribute to postischemic myocardial dysfunction in the intact dog. *Proc. Natl Acad. Sci. USA* **86**, 4695–4699 (1989).
5. Kumar, S., Boehm, J. & Lee, J. C. p38 MAP kinases: key signalling molecules as therapeutic targets for inflammatory diseases. *Nat. Rev. Drug. Discov.* **2**, 717–726 (2003).
6. Lee, J. C. *et al.* Inhibition of p38 MAP kinase as a therapeutic strategy. *Immunopharmacology* **47**, 185–201 (2000).
7. Peifer, C., Wagner, G. & Laufer, S. New approaches to the treatment of inflammatory disorders small molecule inhibitors of p38 MAP kinase. *Curr. Top. Med. Chem.* **6**, 113–149 (2006).
8. Davis, M. E., Hsieh, P. C., Grodzinsky, A. J. & Lee, R. T. Custom design of the cardiac microenvironment with biomaterials. *Circ. Res.* **97**, 8–15 (2005).
9. Christman, K. L. & Lee, R. J. Biomaterials for the treatment of myocardial infarction. *J. Am. Coll. Cardiol.* **48**, 907–913 (2006).
10. Heffernan, M. J. & Murthy, N. Polyketal nanoparticles: A new pH-sensitive biodegradable drug delivery vehicle. *Bioconjug. Chem.* **16**, 1340–1342 (2005).
11. Lee, S. *et al.* Polyketal microparticles: A new delivery vehicle for superoxide dismutase. *Bioconjug. Chem.* **18**, 4–7 (2007).
12. Li, Z. *et al.* Selective inhibition of p38alpha MAPK improves cardiac function and reduces myocardial apoptosis in rat model of myocardial injury. *Am. J. Physiol. Heart Circ. Physiol.* **291**, H1972–H1977 (2006).
13. Liu, Y. H. *et al.* Inhibition of p38 mitogen-activated protein kinase protects the heart against cardiac remodeling in mice with heart failure resulting from myocardial infarction. *J. Card. Fail.* **11**, 74–81 (2005).
14. Minamino, T. *et al.* MEKK1 suppresses oxidative stress-induced apoptosis of embryonic stem cell-derived cardiac myocytes. *Proc. Natl Acad. Sci. USA* **96**, 15127–15132 (1999).
15. Porras, A. *et al.* P38 alpha mitogen-activated protein kinase sensitizes cells to apoptosis induced by different stimuli. *Mol. Biol. Cell.* **15**, 922–933 (2004).
16. Ren, J. *et al.* Role of p38alpha MAPK in cardiac apoptosis and remodeling after myocardial infarction. *J. Mol. Cell. Cardiol.* **38**, 617–623 (2005).
17. See, F. *et al.* p38 mitogen-activated protein kinase inhibition improves cardiac function and attenuates left ventricular remodeling following myocardial infarction in the rat. *J. Am. Coll. Cardiol.* **44**, 1679–1689 (2004).
18. Ding, T., Sun, J. & Zhang, P. Immune evaluation of biomaterials in TNF-alpha and IL-1beta at mRNA level. *J. Mater. Sci.* **18**, 2233–2236 (2007).
19. Iwasaki, Y. *et al.* Reduction of surface-induced inflammatory reaction on PLGA/MPC polymer blend. *Biomaterials* **23**, 3897–3903 (2002).
20. Fernandes, D. C. *et al.* Analysis of dihydroethidium-derived oxidation products by HPLC in the assessment of superoxide production and NADPH oxidase activity in vascular systems. *Am. J. Physiol. Cell. Physiol.* **292**, C413–C422 (2006).
21. Gongora, M. C. *et al.* Role of extracellular superoxide dismutase in hypertension. *Hypertension* **48**, 473–481 (2006).
22. Kim, M. S. *et al.* An in vivo study of the host tissue response to subcutaneous implantation of PLGA- and/or porcine small intestinal submucosa-based scaffolds. *Biomaterials* **28**, 5137–5143 (2007).
23. Davis, M. E. *et al.* Local myocardial insulin-like growth factor 1 (IGF-1) delivery with biotinylated peptide nanofibers improves cell therapy for myocardial infarction. *Proc. Natl Acad. Sci. USA* **103**, 8155–8160 (2006).
24. Widder, J. *et al.* Vascular endothelial dysfunction and superoxide anion production in heart failure are p38 MAP kinase-dependent. *Cardiovasc. Res.* **63**, 161–167 (2004).
25. Zhao, Z. Q. & Vinten-Johansen, J. Myocardial apoptosis and ischemic preconditioning. *Cardiovasc. Res.* **55**, 438–455 (2002).
26. Clerk, A. & Sugden, P. H. Inflame my heart (by p38-MAPK). *Circ. Res.* **99**, 455–458 (2006).
27. Sugden, P. H. & Clerk, A. Oxidative stress and growth-regulating intracellular signaling pathways in cardiac myocytes. *Antioxidants Redox Signal.* **8**, 2111–2124 (2006).
28. Fink, B. *et al.* Detection of intracellular superoxide formation in endothelial cells and intact tissues using dihydroethidium and an HPLC-based assay. *Am. J. Physiol. Cell. Physiol.* **287**, C895–C902 (2004).
29. Sanada, S. *et al.* IL-33 and ST2 comprise a critical biomechanically induced and cardioprotective signaling system. *J. Clin. Invest.* **117**, 1538–1549 (2007).

Supplementary Information accompanies the paper at www.nature.com/naturematerials.

Acknowledgements

The authors wish to thank M. Kemp for her assistance with Bioplex assays for cytokine analysis. This work was supported by a seed grant from Emtech Biotechnology Development (M.E.D.), the Georgia Tech/Emory Center for the Engineering of Living Tissues (funded by NSF-EEC-9731643) (N.M.), NIH UO1 HL80711-01 (N.M.), NIH R21 EB006418 (N.M.), J&J/GT Health Care Innovation Seed Grant Proposal (N.M.) and the Department of Homeland Security (DHS) Scholarship and Fellowship Program, administered by the Oak Ridge Institute for Science and Education (ORISE) through an interagency agreement between the US Department of Energy (DOE) and DHS (J.C.S.). ORISE is managed by Oak Ridge Associated Universities (ORAU) under DOE contract number DE-AC05-06OR23100. All opinions expressed in this paper are the authors' and do not necessarily reflect the policies and views of DHS, DOE or ORAU/ORISE.

Author contributions

The experiments were designed by J.C.S., N.M. and M.E.D., carried out by J.C.S., G.S. and T.O. and interpreted by J.C.S., N.M. and M.E.D. M.B. was responsible for all animal surgeries and echocardiography; S.D. was responsible for design and interpretation of oxidative stress studies as part of the Free Radicals in Medicine Core (FRIMCORE). The manuscript was written by J.C.S., N.M. and M.E.D.

Author information

Reprints and permissions information is available online at http://npg.nature.com/reprintsandpermissions.
Correspondence and requests for materials should be addressed to M.E.D.